Talanta 275 (2024) 126185

Contents lists available at ScienceDirect

Talanta

journal homepage: www.elsevier.com/locate/talanta

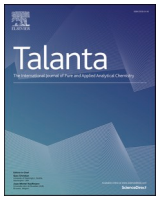

Lab-on kit: A 3D printed portable device for optical and electrochemical dual-mode detection

Cristian Grazioli, Elisa Lanza, Michele Abate, Gino Bontempelli, Nicolò Dossi *

Sustainable Analytical Instrumentation Laboratory (Sustain Lab), Department of Agrifood, Environmental and Animal Science, University of Udine, via Cotonificio 108, I-33100 Udine, Italy

ARTICLE INFO

Handling Editor: Prof. J.-M. Kauffmann

Keywords:
Portable analytical devices
Dual-mode detection
3D printing
Screen printed electrodes
RGB spectrophotometer
Food dyes
Colored candy analysis

ABSTRACT

The hyphenation of electrochemical methods and optical methods in a single portable device is expected to be a challenging combination to enhance the information which can be gained on complex chemical systems. In this paper, a low-cost spectrophotometric device based on low-cost electronics integrated with an electroanalytical cell equipped with a screen printed electrode (SPE) and assembled exploiting a DIY approach, is presented. This easy to use device allowed spectrophotometric and electroanalytical measurements to be performed simultaneously providing simultaneous information and enabling concomitant comparison and autovalidation of the results collected. The analytical robustness and precision of the proposed system was successfully tested on solutions containing mixtures of Patent Blue (E-131) and Brilliant Blue (Erioglaucine E-133), two food dyes displaying optical and redox properties very similar to each other.

1. Introduction

The emerging themes of Green Analytical Chemistry (GAC) and Democratic Analytical Chemistry (DAC) indicate the new perspectives in the field of analytical chemistry aimed at developing innovative methods and devices using economic and environmental sustainable approaches by integrating and sharing multidisciplinary skills [1,2]. The common goals of this new vision include manufacturing cost savings, reduction of energy consumption, waste generation in a profitable and safe way and with better accessibility of the whole population to reliable and on-site useable analytical tools [3]. In particular, considerable efforts are devoted to the development of portable and low-cost miniaturized analytical devices even designed for use by unskilled personnel and also available in remote areas where access to expensive technologies is limited, such as in developing countries [4,5]. The ambitious goal is to make high quality, robust and easy-to-use analytical hardware and software easily available and achievable through widespread manufacturing techniques and projects, in order to enable a wide diffusion of reliable monitoring tools, protocols and point-of-care data acquisition systems [6–8].

In this context, the Open Source concept, which extends from free and open source software (FOSS) to free and open source hardware (FOSH), associated to the Do It Yourself (DIY) approach, the latter implying prototyping or modification of objects even of high technological value, without the intervention of expert personnel, thanks to the sharing and diffusion of information, assembly schemes, projects and instructions on the web, has opened up new and boundless way for the easy assembling of tuneable custom-built analytical devices [9–12]. Against this unprecedented backdrop, scientists and laboratory staff are encouraged to develop powerful research tools, thereby drastically reducing equipment costs. In fact, they can be assembled using readily available materials, components and electronics and can be easily adapted to specific and momentary needs thus overcoming the inaccessibility of conventional instrumentations based on black box systems, with considerable cost savings for research laboratories [13–15]. At the same time, this trend can represent a fascinating opportunity to spread knowledge and to increase interest in analytical chemistry by creating material kits that would make lab science even accessible to remote students.

It is worth noting that the combination of RepRap-class 3D printing and Arduino-based electronics, which are strategic open sources, has been profitably exploited for the construction of user-friendly analytical devices, such as autosamplers, automatic titrators, pH-meters, optical devices or potentiostats that reduce the complexity of manufactoring steps and provide accessible analytical instruments to a wide range of research laboratories with significant economic savings compared to

* Corresponding author.
E-mail address: nicolo.dossi@uniud.it (N. Dossi).

https://doi.org/10.1016/j.talanta.2024.126185
Received 6 December 2023; Received in revised form 23 April 2024; Accepted 28 April 2024
Available online 29 April 2024

equivalent or less functional proprietary instruments [16–23]. In addition, these manufactoring techiniques offer great potential to assemble modular units which can be combined into hybrid systems in order to benefit from the advantages or, if necessary, to overcome the limitation of using only one of them.

The detection of several analytes can be performed by exploiting more than one of their properties. Thus, for instance, food dyes not only display defined absorption spectra in the visible range, but are almost all electroactive [24–28]. Therefore, the hyphenation of electrochemical methods and optical methods, both displaying remarkable analytical performance and easy miniaturization, is expected to be a challenging combination to improve the information which can be gained on samples containing simultaneously these dyes [28–33]. Following this reasoning, the availability of portable dual signal analytical systems that allow simultaneous optical and electrochemical readout can improve detection and provide self-verification, thus improving both accuracy and reliability of measurements.

This article describes a customizable and robust spectrophotometric device based on an Arduino microcontroller assembled exploiting 3D printing technology and inexpensive electronic components such as light-emitting diodes (LEDs) and phototransistors. This device is integrated with an electroanalytical cell equipped with a screen printed electrode (SPE), thus allowing spectrophotometric and electroanalytical measurements to be performed simultaneously.

As a proof-of-concept, the performance of this highly versatile device was tested on solutions containing mixtures of Patent Blue V (E-131) and Brilliant Blue (Erioglaucine E-133), two food dyes displaying both optical absorbance in the visible region and redox properties very similar to each other, carefully choosing the optimal experimental conditions and the instrumental parameters to be used for their selective determination.

2. Materials and methods

2.1. Chemicals

Ultrapure water (>18 MΩ cm) was obtained from a PURELAB UHQ (ELGA, UK) system. Patent Blue V (PB, E-131), Brilliant Blue FCF (Erioglaucine, BB, E-133), potassium chloride, potassium hydrogen phthalate, phthalic acid, sodium acetate, sodium dihydrogen phosphate, sodium hydrogen phosphate, sodium tetraborate decahydrate, hydrochloric acid, phosphoric acid, acetic acid and sodium hydroxide were purchased from Sigma-Aldrich (Sigma-Aldrich, Milan, IT). The solution at pH 2 was prepared using HCl at a concentration of 0.01 M. 0.1 M buffer solutions at increasing pHs (2,5, 3; 4.5; 7; 8.5) were prepared using the above mentioned compounds. KCl was added to all solutions to achieve a final chloride ion concentration equal to 0.2 M.

Standard solutions of PB and BB were prepared in water at concentrations of 20 mM and subsequently diluted in the used electrolytic solution to achieve the desired concentrations (2–200 μM).

Spectrophotometric measurements were also performed with a benchtop spectrophotometer (Varian Cary 50 bio, Victoria, AUS) using polymethylmethacrylate cuvettes with an optical path of 1 cm. Preliminary voltammetric measurements were carried out in a conventional cell (5 mL) using a glassy carbon working electrode, a platinum counter electrode and an Ag/AgCl, 3 M KCl reference electrode. Electrochemical measurements in the miniaturized apparatus were made using a SPE device (DS-110, Metrohm, Varese, IT) assembled with electrodes printed with graphite-based (for working and counter electrodes) or silver-based (for the reference electrode) inks.

All electrochemical measurements were carried out using a potentiostat (CH Instruments, Austin, TX, USA).

2.2. Assembly of the portable device for simultaneous electrochemical and spectrophotometric measurements

A portable device, enabling simultaneous electrochemical and absorbance measurements, was assembled using low-cost electronic components and open source technology. It consisted of a plastic box made up of two ABS (Acrylonitrile Butadiene Styrene) frames, one front and one rear, which were fitted together and secured with four screws. Both frames were built using a FLSUN Cube 3D printer and a FUSION 360 software to design the components to be printed. As shown in Fig. 1a, this box was equipped with an external fluidic consisting of inlet and outlet silicone tubes connected to a syringe for the filling operation and to a waste container, respectively. The device also included an internal fluidics that allows both the transfer of the analyzed sample from the inlet to the two detection zones and a suitable housing for the electronic components (LEDs and phototransistor) and the SPE electrode. This device was composed by several components that were easily assembled following simple instructions (lab-on kit). Two transparent circular windows made of a thin polyvinylchloride (PVC) film (180 μm thick) were attached to the ABS frame to separate the liquid from the optical detection zone in correspondence with the holes created for the exit and reception of the light beam (see Fig. 1b for the front frame and Fig. 1e for the rear frame). The hydraulic seal of the circuit was assured by the use of an hexagonal rubber gasket and an O-ring (see Fig. 1c, d and 1e). PVC windows and hexagonal shaped rubber seals were made using a cutting plotter (Silhouette CAMEO, Micronet Italia, Milan, Italy).

The dimensions of the device were the following: height 5 cm, thickness 2 cm, width 3 cm. The optical path of the cell for spectrophotometric detections was 0.3 cm and the electroanalytical sensing zone was defined by the walls of the O-ring (8 mm) which also allowed the SPE to be locked in a fixed position. The volume available in this last zone was 50 μL, which allowed the three electrodes present in the SPE to be completely wetted.

The light source used was a KY-009 RGB module within which three different LEDs were integrated (5050 SMD LED), these last capable of emitting different light radiations at three distinct small wavelength intervals (RGB LED): red (R) 620–635 nm; green (G) 500–530 nm; blue (B) 460–475 nm. A module with a n-p-n type phototransistor (TEMT6000), with an integrated voltage divider, was used as the detector (see Fig. 1c and d). Both source and detector were connected to the Arduino board which was in turn connected to a PC through an USB port, used for both its power supply (5 V) and data communication (see Fig. 1f). In particular, three of the four pins present in the module used as the light source and corresponding to the RGB channels were connected to the digital pins (2-3-4, anodes) of the board, while the fourth pin was connected to the GND pin (ground, cathode). The three pins present in the phototransistor module were instead connected to the output pin, capable of supplying a voltage of 5 V, to the second GND pin and to the analogic input pin (A0), respectively. Through this last input pin, the analogic signal (voltage) coming from the phototransistor and dependent on the intensity of the incident light beam (therefore on the analyte concentration) was acquired by the Arduino board, converted into a digital signal and transferred to the PC for data visualization.

2.3. Procedures followed for spectrophotometric and electroanalytical detection with the portable device

A 20 mL syringe was used for filling analyzed solutions and for washing with water, paying particular attention to avoid the possible formation of bubbles. A three-way valve, placed at the outlet of the device in the terminal part of the silicone tube, allowed the opening and closing of the fluidic circuit during the different steps, i.e. filling, analysis, emptying and cleaning. Before analysis of a new solution, three consecutive washings with water were carried out in order to guarantee the maximum cleanliness of the device fluidic. The fluid leaving the device was collected in a waste container. Both spectrophotometric and

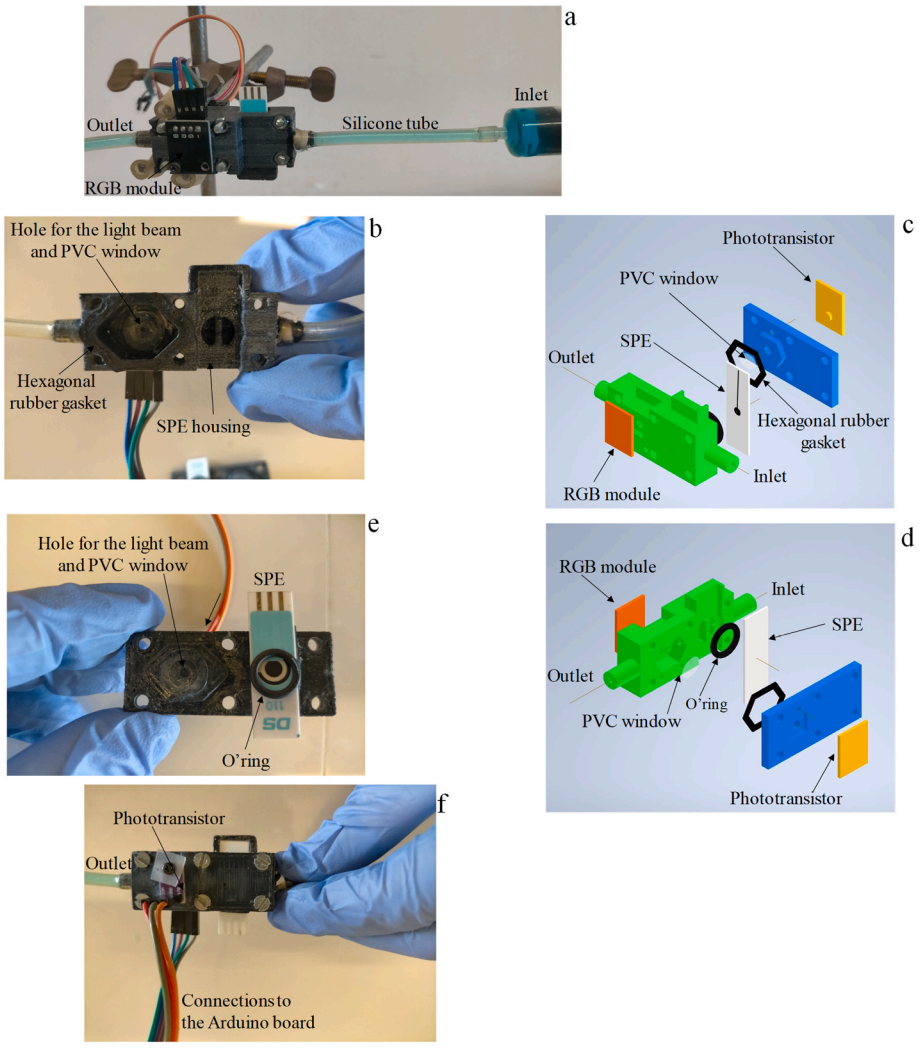

Fig. 1. Pictures and schemes of the 3D printed device housing the optical and electrochemical detection zones: (a and f) front and rear view of the assembled device; (b and e) inner parts of the disassembled ABS frames; (c and d) exploded views and schemes of the individual parts.

electrochemical measurements were performed under static conditions.

The acquisition of spectrophotometric data were managed by the Arduino software, using a properly written code in C++ language that allowed to calculate transmittance and absorbance values of the analyzed solutions at the three different light radiations emitted by the RGB module. A first reading was performed using an analyte-free buffer solution, thus achieving a value that was automatically stored and displayed in the PC as the blank. Subsequently, dye solutions with increasing concentrations were introduced and 5 absorbance readings were performed, one after the other, at each of the three different wavelengths. The average value of these measurements, from which the blank value was automatically subtracted, was finally displayed on the PC.

Electrochemical measurements were performed on the same solutions using the SPE electrode positioned in the corresponding EC detection zone.

2.4. Real sample preparation

Chocolate pellets with colored shell subjected to analysis were purchased from local supermarkets. Before analysis, colored candies (about 3 g) were simply dipped for about 2 min in 4 mL of sodium phosphate (0.1 M; pH = 2.5), in order to dissolve the external colored coating. The obtained solutions were then centrifuged (5200 rpm, 3 min), filtered with 0.45 μM filters (Gelman Acrodisc) and subsequently diluted 1:8 with the mentioned electrolytic solution. Since these analyzed candies were colored with only one of the two dyes considered here (BB), controlled amounts of the other dye (PB) were added to these solutions after filtration.

3. Results and discussion

3.1. Spectrophotometric measurements with a conventional spectrophotometer

Spectrophotometric investigations were preliminarily conducted using a conventional benchtop instrument in order to evaluate the pH effect on the spectral behavior of the two similar triarylmethane food dyes here considered. These measurements were carried out using buffer solutions at different pH (2; 2.5; 3; 4.5; 7.0; 8.5).

As already highlighted by other authors [34], Patent Blue V (PB) is an acid-base indicator whose color changes from yellow (pH 0.8) to blue (pH 3), on passing through a series of shades between yellow and green that accompany the variation of the H_3O^+ concentration.

Accordingly, our spectrophotometric measurements showed that a progressive decrease of the band with a maximum absorption at about 640 nm took place on passing from pH 2 to pH 3 in a 10 μM PB solution, which is accompanied by the appearance and progressive increase of an

absorption band with a maximum at about 415 nm, as shown in Fig. 2a.

Similar measurements conducted on Brilliant Blue (BB), which is also a triarylmethane dye widely used in the food industry, showed instead a different behavior. In fact, the BB spectrum, which consists of a main band at 630 nm and a modest band at 410 nm, remained practically unchanged in the pH range 2–3, as shown in Fig. 2b, since the acid-base involving the transition from yellow to blue is shifted to more acidic pH, as reported in the literature [35] (pH < 1.0).

This different spectral behavior displayed by the two dyes at pH 2 and 2.5 suggested that it could be useful for the selective determination of PB even in the presence of BB. In addition, this preliminary investigation confirmed the possibility of using a simple detection system assembled with a low cost light source (RGB LED) capable of emitting in three different range of wavelength of the visible region (red (R) 620–635 nm; green (G) 500–530 nm; blue (B) 460–475 nm) and a phototransistor to acquire optical signals, in particular those relative to the red and blue channels.

3.2. Voltammetric measurements in a conventional electrochemical cell

The electrochemical behavior of PB in the media where the spectral differences were observed (buffer solutions at pH 2, 2.5 and 3) was preliminarily investigated also by cyclic voltammetry using a conventional three-electrode cell.

As it can be observed in the voltammetric profiles reported in Fig. 3a in the pH range 2–3, PB was characterized by an anodic peak (Ep_a = 0.84 V) associated to a cathodic peak, recorded in the backward scan (Ep_c = 0.79 V), typical of a reversible process. It is worth noting that, under these experimental conditions no passivation phenomena of the working electrode surface (fouling) was observed even when voltammetric scans were performed repeatedly.

However, this voltammetric profile for PB changed progressively when the pH was increased over 3 (not reported in Fig. 3), until it reached a voltammetric profile consisting of the sole oxidation peak at Ep_a = 0.84 V, thus assuming a typically irreversible profile. This behavior can be explained on considering that, as reported for several triphenylmethane dyes [36,37], the anodic process for PB occurs through an electron transfer involving one of the two dimethylamino groups present in its molecule. This charge transfer causes the formation of a radical cation whose stability in acid media (pH < 3) is sufficiently high, so as to allow the occurrence of its cathodic reduction to be observed in the reverse scan. Only at lower H_3O^+ concentrations (pH > 3) the electron transfer is followed by the release of a proton in a chemical reaction which becomes more rapid.

Voltammetric measurements conducted on the BB dye, showed instead that the oxidation of this dye displayed a partial reversibility only at pH 2, while at pH 2.5 and 3 only one anodic peak at Ep_a = 0.95 V is observed with no associated return peak. This can be explained by considering that the chemical reaction following the electron transfer for BB is faster at these pHs with respect to that for PB, just in view of the fact that its acid-base constant is significantly lower for this dye, as mentioned in the previous section.

The different electrochemical behavior observed in these preliminary studies for the two dyes suggested that the aqueous solution at pH = 2.5 could be an optimal candidate as supporting electrolyte for the EC detection of PB even in the presence of BB.

This different behavior was also observed in the measurements made subsequently using differential pulse voltammetry (DPV), which allows to eliminate the contribution of the capacitive current, which is not directly connected to the redox process of the investigated species, thus increasing the measurement sensitivity. The parameters for DPV were optimized using a PB solution at a concentration of 0.5 mM and resulted to be: scan range (0–1.1 V); pulse increase (0.004 V); pulse width (0.1 V); pulse duration (0.15 s); sampling time (0.02 s); pulse period (0.6 s).

The DPV profiles shown in Fig. 4 for the two dyes at the same concentration (500 μM) showed a higher peak current for PB with respect to that recorded for BB, in agreement with the different degree of reversibility displayed in their different electrochemical processes.

3.3. Response of the portable device for solutions containing each single dye

This investigation was aimed at evaluating the performance offered by this dual-mode detection device in analysis of solutions containing simultaneously two species displaying quite similar optical and electroanalytical properties, such as the two dyes PB and BB. For this purpose, it is obviously necessary to know preliminarily the behavior displayed individually by each component. Therefore, some tests were first conducted on each dye introduced separately in the proposed device.

The performance of the device in terms of repeatability of the signals collected at the three different light sources available and at the SPE were evaluated using a 10 μM solution of either PB or BB dissolved in a buffer solution at pH 2.5. With this purpose, absorbance values, indicated as $A_{R(620\text{-}635\ nm)}$, $A_{G(500\text{-}530\ nm)}$, $A_{B(460\text{-}475\ nm)}$, and voltammetric profiles were recorded using the same dye solutions in 7 repetitive measurements. DPV experiments at the SPE were carried out adopting the parameters previously optimized in the conventional cell and reported in Section 3.2. Under these conditions, PB exhibited an anodic profile characterized by a single peak (Ep_a = 0.62 V), as shown in Fig. 5a, while BB displayed a single anodic peak (see Fig. 5b) at a slightly higher potential (Ep_a = 0.72 V).

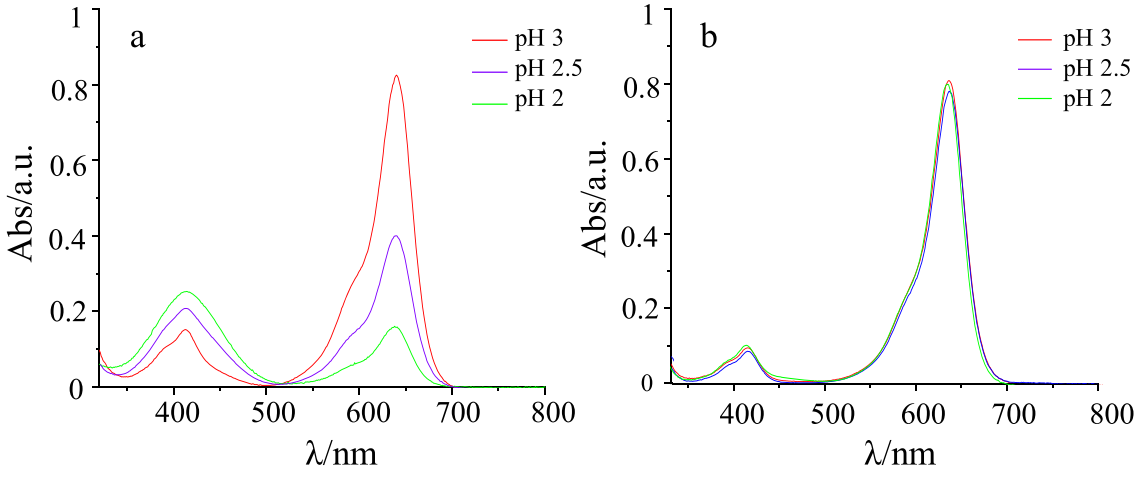

Fig. 2. Visible spectra recorded with a conventional spectrophotometer for 10 μM PB (a) and BB (b) dissolved in buffer solutions at pH 2, 2.5 and 3.

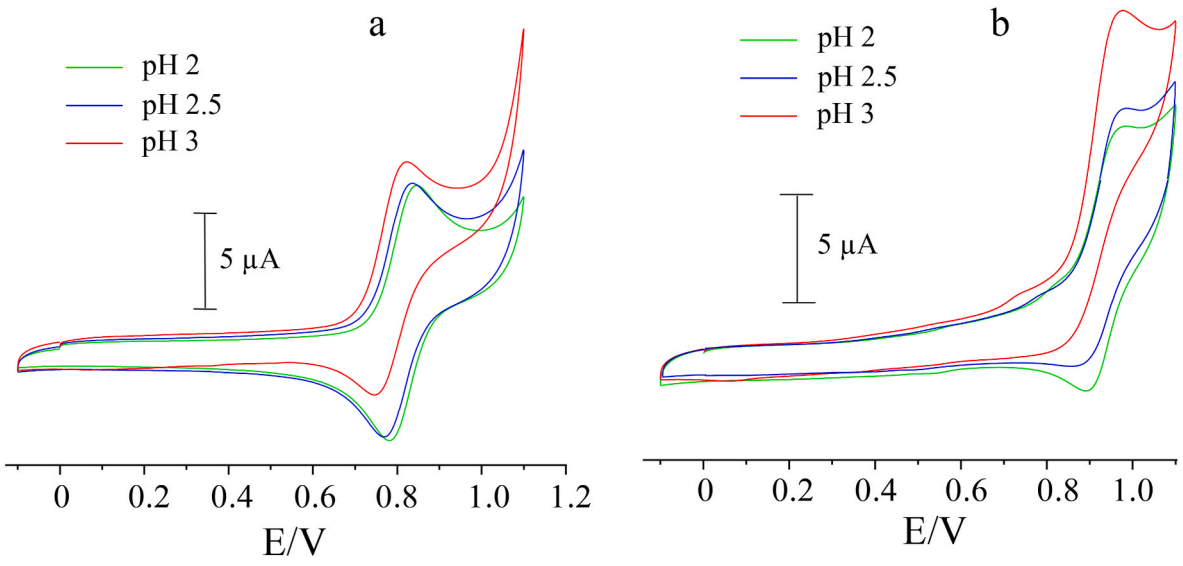

Fig. 3. Cyclic voltammetric profiles recorded at a glassy carbon electrode *vs* a Ag/AgCl reference electrode for a 1 mM PB (a) and BB (b) dissolved in buffer solutions at pH 2, 2.5 and 3. Scan rate 50 mVs^{-1}.

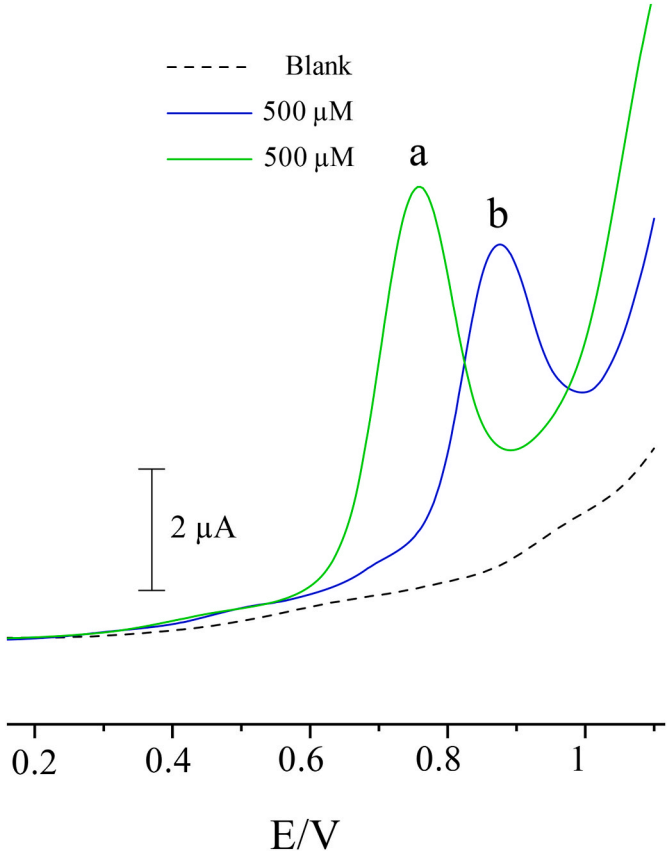

Fig. 4. DPV profiles recorded at a glassy carbon electrode *vs* a Ag/AgCl reference electrode in a conventional cell for solutions containing 500 µM of PB (a) and BB (b) in a phosphate buffer at pH = 2.5.

Once again, no electrode passivation (fouling) could be observed even when voltammetric scans where repeatedly performed. Peak currents recorded in these voltammetric measurements showed optimal repeatability (RSD ≤ 1.8) and a good repeatability (≤2.6 %) was also found for absorbance measurements, regardless the wavelength considered.

It must be underlined that repeated tests performed with this dual-mode detection device require some washing operations, syringe connection and insertion, as well as removal of the SPE electrode used for the electrochemical detection. Consequently, a series of repeated tests were also carried out, using the same reference samples (PB or BB 10 µM) to evaluate the reproducibility involved in these reassembly operations, once again based on peak currents and absorbance values. The results obtained showed that these operations led for both dyes to relative standard deviations (RSD ≤ 2.8 and ≤ 3.1 % for EC and optical measurements, respectively) only a little bit higher than the repeatability mentioned previously.

Finally, by using solutions of PB and BB at increasing concentrations, introduced separately, it was possible to construct calibration plots by using both the height of the DPV peaks at 0.62 V and 0.72 V for PB and BB, respectively and the absorbances recorded at the three light sources available (R, G and B).

The calibration plots constructed by DPV peaks for both dyes were characterized by a satisfactory linearity in the concentration range considered (2–200 µM) and their regression equations were as follows: i $(\mu A)_{620mV}$ = 0.0039 C (µM) + 0.0630; R^2 = 0.98 and i $(\mu A)_{720mV}$ = 0.0168 C (µM) + 0.2627; R^2 = 0.99 for BB and i $(\mu A)_{620mV}$ = 0.0242 C (µM) + 0.2992; R^2 = 0.99 and i $(\mu A)_{720mV}$ = 0.0053 C (µM) + 0.2092, R^2 = 0.98 for PB, respectively.

A satisfactory linearity was also found for the calibration plots constructed using absorbance values collected at the three wavelengths emitted by the light source for solutions containing the two dyes individually in the concentration range (2–100 µM), as shown in Fig. 6 where their regression equations are also reported.

3.4. Dual-mode detection of solutions containing both PB and BB

Solutions containing the two dyes PB and BB at a total concentration of 100 µM but in different ratios were prepared on purpose and analyzed by recording simultaneously optical and DPV signals.

For all these solutions the optical signals recorded as absorbance (A) and the peak currents (i_p) recorded in the differential pulse voltammograms were expected to result from the additive contribution of the two dyes. However, the information gained previously as $A_{R(620\text{-}635\ nm)}$, $A_{G\ (500\text{-}530\ nm)}$, $A_{B(460\text{-}475\ nm)}$ suggested that the spectral data were poorly suited to allow a distinction of the two dyes, while the electroanalytical data were expected to provide the possibility to better distinguish the contents of PB and BB, since the corresponding signals were to some

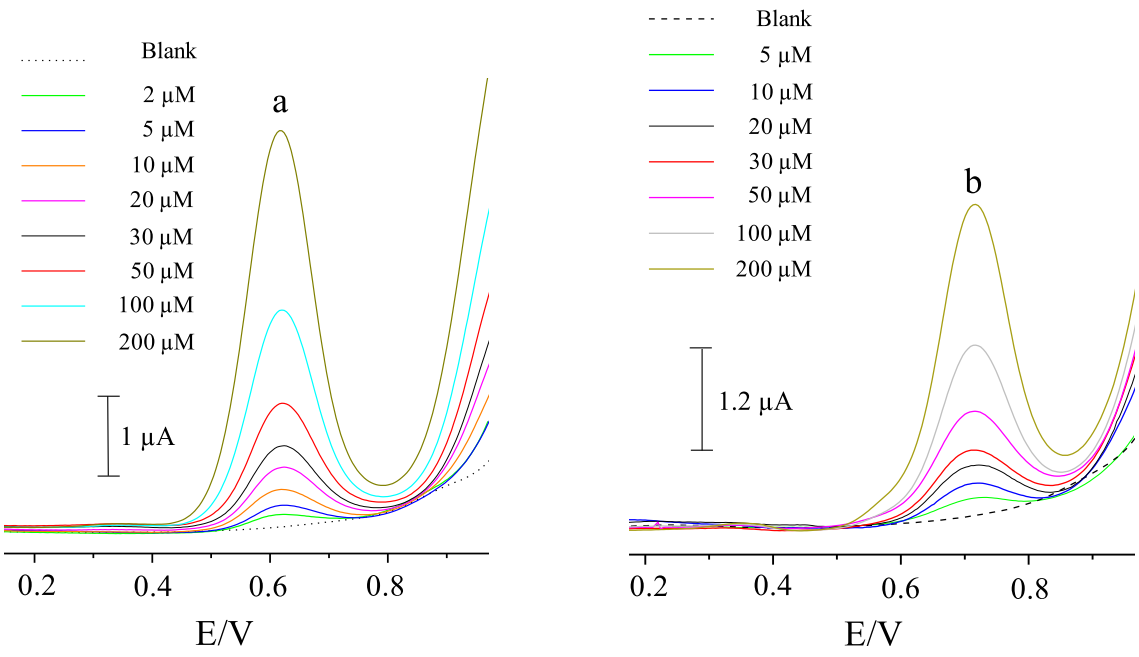

Fig. 5. DPV profiles recorded at a SPE for solutions containing increasing concentrations of PB (a) and BB (b) in a phosphate buffer at pH = 2.5.

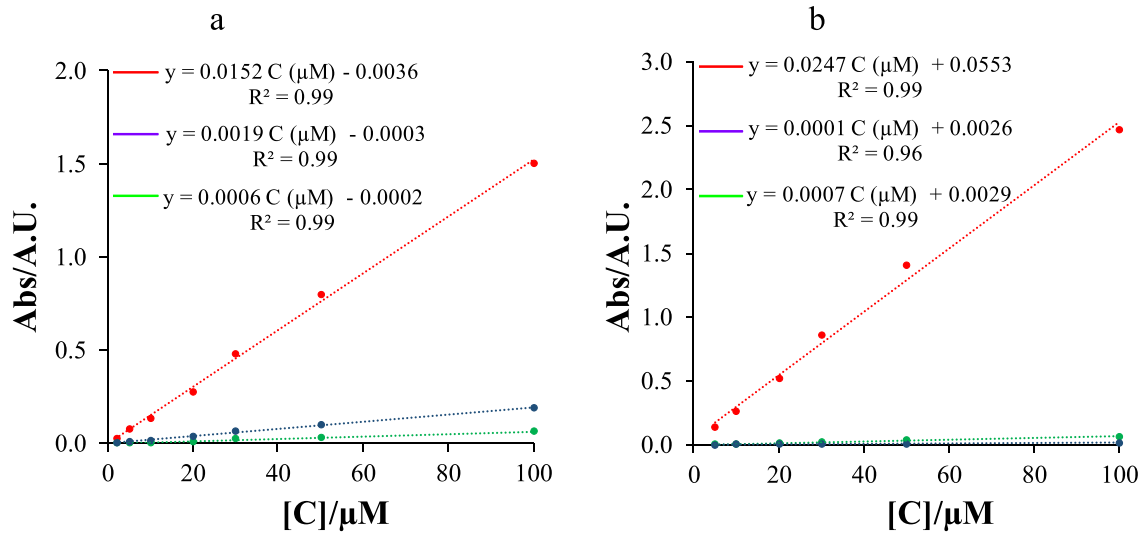

Fig. 6. Calibration plots constructed at the red (R, 620–635 nm), green (G, 500–530 nm), blue (B, 460–475 nm) channels for Patent Blue (a) and Brilliant Blue (b).

extent different from each other, as shown in Fig. 7.

In order to verify whether the signals recorded using the two approaches adopted were able to provide a more or less satisfactory quantification of PB and BB simultaneously present in the same solutions, the signals detected in each of the prepared mixtures were used to calculate the concentrations of the two dyes, which were then compared with those actually introduced.

As to absorbance measurements, $A_{R(620\text{-}635\ nm)}$, $A_{B(460\text{-}475\ nm)}$, recorded using the R and B light sources were used because they were expected to provide better sensitivity and selectivity with respect to signals recorded at the G channel. BB and PB concentrations were hence calculated by solving the equation system reported below, written on the basis of the law of the additivity of spectroscopic absorbances [38,39] (see the regression equations reported in Fig. 6).

(B channel) $A_{B(460\text{-}475\ nm)} = 0.0001C_{BB}(\mu M) + 0.0019C_{PB}(\mu M)$

(R channel) $A_{R(620\text{-}635\ nm)} = 0.0247C_{BB}(\mu M) + 0.0152C_{PB}(\mu M)$

In these equations the independent term required to account for a non-zero intercept was omitted because the single intercepts found are relatively modest (see Fig. 6) and furthermore the background signals responsible for the global intercept were expected to overlap each other.

The concentrations thus calculated were then compared with the expected concentrations, $C_{expected}$, in Table 1, where also the corresponding percent errors (σ%) are reported, these latter calculated as:

$\sigma\% = 100\ (C_{found} - C_{expected}) / C_{expected}$

As expected, the results obtained provided only a very crude

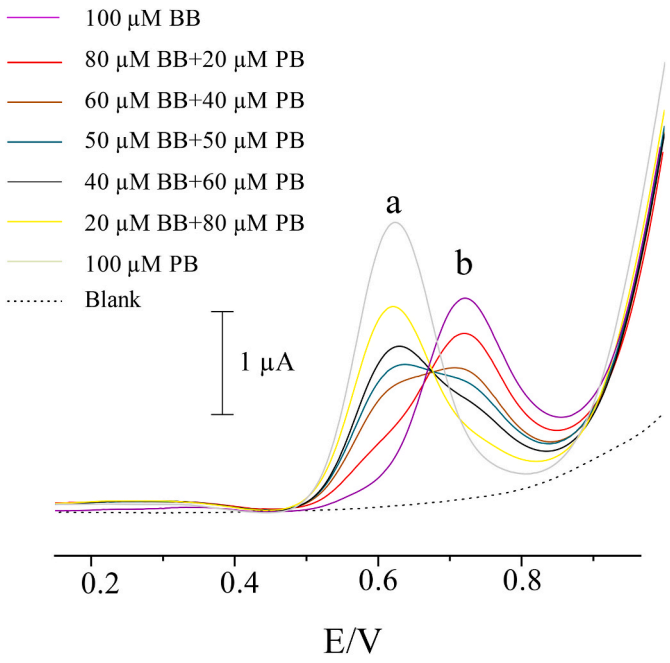

Fig. 7. DPV responses recorded at a SPE for phosphate buffered solutions (pH = 2.5) simultaneously containing PB (a) and BB (b) at the indicate concentrations.

discrimination of the two dyes mixed together, because they were obtained from spectral signals detected at wavelengths at which both dyes display an almost equal absorbance.

The same calculation procedure was adopted using the peak currents recorded by DPV in the mentioned mixtures of PB and BB at 620 mV and 720 mV. Thus, peak heights recorded at 620 and 720 mV for each of the prepared mixtures were inserted in the equations system reported below, exploiting the regression equations found at the mentioned potentials for each of the two dyes and reported in the previous Section. Also in this case, the independent term required to account for a non-zero intercept was omitted.

$$i_p\ 620\ mV = 0.0039\ C_{BB}(\mu M) + 0.0242 C_{PB}(\mu M)$$

$$i_p\ 720\ mV = 0.0168 C_{BB}(\mu M) + 0.0053 C_{PB}(\mu M)$$

Once again, the concentrations thus calculated were then compared with the expected concentrations, $C_{expected}$, in Table 1, where also the percent errors σ% are reported, these latter calculated as reported above.

As it was expected, better results, characterized by small errors, were found by electroanalytical measurements. Nevertheless, also the results collected by absorbance measurements were to some extent consistent, thus showing that the combined use of the two approaches might offer some advantage.

3.5. Analysis of real samples

In order to evaluate the applicability of the analytical system here described, analyses of two different colored candies were carried out. The samples were chosen based on what was indicated on their label. Unfortunately, samples containing simultaneously the two dyes were not commercially available. Consequently, two samples containing the sole BB were used for our purpose. The BB concentration in these samples, determined by us as the mean values of measurements carried out both voltammetrically (720 mV) and spectrophotometrically (R channel) turned out to be about 19.1 μM in the first sample and 17.3 μM in the second sample, with deviations which did not go beyond ±7 %.

Since sample labels reported that the coating of the colored candies consisted essentially of sucrose and other polysaccharides, which are chemical species unable to undergo anodic oxidation under our experimental conditions and to display absorption bands in the ranges explored, no appreciable interference was expected. However, the possible matrix effect on our determinations was at first estimated by performing measurements on candies after addition of known amounts of BB, in order to achieve additional concentrations equal to 20, 30 and 50 μM. The difference between the heights of the anodic DPV peak and absorbances recorded after these standard additions and that of the peak before supplementation were then compared with the calibration plots constructed for the pure BB dye. The results of these preliminary tests enabled to evaluate that under these conditions, during DPV measurements the determined BB concentrations were equal to about 91.2 % of those actually added and that a quite similar deviation (89.2 %) was found by conducting spectrophotometric measurements on the same supplemented real samples.

Finally, measurements on real samples were performed after addition of known amounts of PB, in order to achieve concentrations of this dye equal to 20, 30 and 50 μM in both the two samples containing BB. Simultaneous voltammetric and spectrophotometric quantification of BB and PB in these real samples, performed in triplicate (N = 3) using the previously described approach, was applied to these different samples. The results, affected by errors comparable to those previously obtained, are reported in Table 2.

4. Conclusions

In this paper, the development of a hybrid sensing platform suitable for simultaneous optical and electrochemical detection and capable of offering the advantages of each individual technique is presented.

The entire device can be easily assembled at very low-cost by equipping a suitable 3D printed plastic holder, containing an internal fluidic connecting two separated detection zones with a commercial screen printed electrode and a customized spectrophotometer consisting of a RGB light source, an optical photodetector, an Arduino microcontroller and a software for data acquisition and signal processing. A key advantage of this device consists in the possibility to assemble modular units and separate parts which may easily managed independently or simultaneously for the measurement of the light absorption associated to

Table 1
Comparison of the concentrations found by using the equation systems written for both optical and DPV measurements with the expected concentrations (solutions prepared on purpose), together with the relevant percent errors (σ%).

Expected		Found by spectrophotometric measurements				Found by DPV measurements			
C_{BB} (μM)	C_{PB} (μM)	C_{BB} (μM)	σ%	C_{PB} (μM)	σ%	C_{BB} (μM)	σ%	C_{PB} (μM)	σ%
100	0	92.8	−7.2	11.1	∞	113.0	13	0.86	∞
80	20	74.2	−7.2	30.5	52.5	88.1	10.2	17.4	−13.1
60	40	56.6	−5.6	48.8	22.0	61.6	2.7	37.6	−6.1
50	50	44.3	−11.5	57.6	15.2	52.3	4.7	46.5	−6.9
40	60	34.6	−13.4	66.8	11.3	39.5	−1.2	56.4	−5.9
20	80	11.7	−41.4	86.6	8.3	18.7	−6.5	76.1	−4.9
0	100	10.9	∞	104.5	4.5	2.71	∞	104	3.8

Table 2
Concentration values of the two dyes determined in the analysis of the two real samples supplemented with controlled amounts of PB, together with the relevant RSD% (N = 3).

Expected		Found by spectrophotometric measurements				Found by DPV measurements			
C_{BB} (μM)	C_{PB} (μM)	C_{BB} (μM) Mean	RSD%	C_{PB} (μM) Mean	RSD%	C_{BB} (μM) Mean	RSD%	C_{PB} (μM) Mean	RSD %
19.1	20	15.9	4.9	22.3	5.1	22.1	3.2	17.4	2.6
19.1	30	16.3	6.1	34.1	5.8	22.3	2.4	26.3	2.1
19.1	50	16.8	4.1	56.6	5.2	21.9	2.1	47.4	2.8
17.3	20	14.1	4.3	22.9	4.8	19.3	3.6	18.1	1.9
17.3	30	14.9	5.2	32.3	5.3	19.8	3.9	27.3	2.3
17.3	50	14.8	5.9	54.4	3.8	18.2	2.9	48.1	3.1

analytes present in the analyzed samples and the current intensity or potential peak position related to the electrochemical processes occurring at the surface of a working electrode.

As a proof-of-concept, the presented platform was applied to the determination of two commonly used food dyes and for investigating their mixtures.

The simultaneous availability of electroanalytical and spectrophotometric data make possible the construction of two different calibration plots relative to two independent signals for controlling whether a significant concentration difference is found between the two types of measurements, thus avoiding undesirable and incorrect results or overcoming some possible limitation affecting one of the two employed techniques, such as a limited quantification range, passivation problems of the electrode surface or excessive sample turbidity.

It is believed that this multiple-detection strategy can provide significant improvements in analytical efficiency and precision, compared to single-mode detection, and may open a new path in the development of sensing devices. The use of RGB LEDs presented in this work may extend the potential number of applications and at the same time provides multiple signals to be recorded which could be exploited for the discrimination of multiple analytes on the basis of their absorption properties. In addition, the fluidic systems make possible the easy change of solutions and the possible use of different reactants in order to modify the electrode surface or needed to exploit specific chemical, enzymatic and colorimetric reactions.

In order to acquire complementary information [28], electroanalytical measurements are quite often coupled with relatively sophisticated spectral measurements, such as fluorometric, SERS and SPR, but also with simple colorimetric measurements. However, very often these measurements are conducted in parallel with different benchtop instrumentation [29], even though there are examples where these combined measurements are made simultaneously and ordinary tools such as smartphones are used for reflectance signal acquisition [30]. Despite this approach is interesting, it may suffer from a lack of sensitivity compared to transmittance measurements and the use of smartphones suffers from some limitations due to the variability of sensors and processing algorithms used in the image digitization used in different models [22].

Recently, an interesting approach was proposed using a photometer consisting of a far red light emitting diode and a Si photodiode detector combined with a screen printed transparent nanopaper for the dual opto-electrochemical determination of acetominophen based on the formation of Prussian Blue [32].

CRediT authorship contribution statement

Cristian Grazioli: Software, Investigation, Formal analysis, Data curation. **Elisa Lanza:** Methodology, Investigation, Data curation. **Michele Abate:** Investigation, Formal analysis, Data curation. **Gino Bontempelli:** Writing – review & editing, Formal analysis, Data curation. **Nicolò Dossi:** Writing – review & editing, Writing – original draft, Methodology, Funding acquisition, Formal analysis, Data curation, Conceptualization.

Declaration of competing interest

The authors declare that they have no known competing financial interests or personal relationships that could have appeared to influence the work reported in this paper.

Data availability

No data was used for the research described in the article.

References

[1] E. Vidal, A.S. Lorenzetti, F.J.V. Gomez, M.F. Silva, C.E. Domini, Brand new dual absorption and emission smartphone-based spectrophotometer (DAESS) for the study of the role of water in the preparation of natural deep eutectic solvents, Anal. Chim. Acta 1179 (2021) 338831, https://doi.org/10.1016/j.aca.2021.338831.
[2] F. Chemat, S. Garrigues, M. de la Guardia, Portability in analytical chemistry: a green and democratic way for sustainability, Curr. Opin. Green Sustainable Chem. 19 (2019) 94–98, https://doi.org/10.1016/j.cogsc.2019.07.007.
[3] P. Aryal, E. Brack, T. Alexander, C.S. Henry, Capillary flow-driven microfluidics combined with a paper device for fast user-friendly detection of heavy metals in water, Anal. Chem. 95 (2023) 5820–5827, https://doi.org/10.1021/acs.analchem.3c00378.
[4] M. de la Guardia, S. Garrigues, Past, present and future of green analytical chemistry, in: S. Garrigues, M. de la Guardia (Eds.), Challenges in Green Analytical Chemistry, second ed., The Royal Society of Chemistry, 2020, pp. 1–18, https://doi.org/10.1039/9781788016148-00001. Ch. 1.
[5] P. Aryal, E. Brack, T. Alexander, C.S. Henry, Capillary flow-driven microfluidics combined with a paper device for fast user-friendly detection of heavy metals in water, Anal. Chem. 95 (2023) 5820–5827, https://doi.org/10.1021/acs.analchem.3c00378.
[6] J.F. Bergua, I.R. Á lvarez-Diduk, I.A. Idili, C. Parolo, M. Maymó, L. Hu, A. Merkoçi, Low-cost, user-friendly, all-integrated smartphone-based microplate reader for optical-based biological and chemical analyses, Anal. Chem. 94 (2022) 1271–1285, https://doi.org/10.1021/acs.analchem.1c04491.
[7] K.E. Boehle, E. Doan, S. Henry, J.R. Beveridge, S.L. Pallickara, C.S. Henry, Single board computing system for automated colorimetric analysis on low-cost analytical devices, Anal. Methods 10 (2018) 5282, https://doi.org/10.1039/c8ay01874j.
[8] N. Jiang, N.D. Tansukawat, L. Gonzalez-Macia, H.C. Ates, C. Dincer, F. Güder, S. Tasoglu, A.K. Yetisen, Low-cost pptical assays for point-of-care diagnosis in resource limited settings, ACS Sens. 6 (2021) 2108–2124, https://doi.org/10.1021/acssensors.1c00669.
[9] H.R. Singhal, A. Prabhu, G. Nandagopal, T. Dheivasigamani, N. Kumar Mani, One-dollar microfluidic paper-based analytical devices: do-it-yourself approaches, Microchem. J. 165 (2021) 106126, https://doi.org/10.1016/j.microc.2021.106126.
[10] M.D.M. Dryden, R. Fobel, C. Fobel, A.R. Wheeler, Upon the shoulders of giants: open-source hardware and software in analytical chemistry, Anal. Chem. 89 (2017) 4330–4338.
[11] M. Caux, A. Achit, K. Var, G. Boitel-Aullen, D. Rose, A. Aubouy, S. Argentieri, R. Campagnolo, E. Maisonhaute, PassStat, a simple but fast, precise and versatile open source potentiostat, HardwareX 11 (2022) e00290, https://doi.org/10.1016/j.ohx.2022.e00290.
[12] O. Rodríguez, M.A. Pence, J. Rodríguez-López, Hard potato: a Python library to control commercial potentiostats and to automate electrochemical experiments, Anal. Chem. 95 (2023) 4840–4845, https://doi.org/10.1021/acs.analchem.2c04862.
[13] A. Tonelli, A. Candiani, M. Sozzi, A. Zucchelli, R. Foresti, C. Dall'Asta, S. Selleri, A. Cucinotta, The geek and the chemist: antioxidant capacity measurements by DPPH assay in beverages using open source tools, consumer electronics and 3D printing, Sens. Actuators, B 282 (2019) 559–566, https://doi.org/10.1016/j.snb.2018.11.019.
[14] N. Dossi, F. Terzi, E. Piccin, R. Toniolo, G. Bontempelli, Rapid prototyping of sensors and conductive elements by day-to-day writing tools and emerging manufacturing technologies, Electroanalysis 28 (2016) 250–264, https://doi.org/10.1002/elan.201500361.

[15] B. Hemmateenejad, E. Rafatmah, Z. Shojaeifard, Microfluidic paper and thread-based separations: chromatography and electrophoresis, J. Chromatogr. A 1704 (2023) 464117, https://doi.org/10.1016/j.chroma.2023.464117.
[16] A. Ambrosi, A. Bonanni, How 3D printing can boost advances in analytical and bioanalytical chemistry, Microchim. Acta 188 (2021) 265, https://doi.org/10.1007/s00604-021-04901-2.
[17] H. Agrawaal, J.E. Thompson, Additive manufacturing (3D printing) for analytical chemistry, Talanta Open 3 (2021) 100036, https://doi.org/10.1016/j.talo.2021.100036.
[18] R. Toniolo, N. Dossi, E. Giannilivigni, A. Fattori, R. Svigelj, G. Bontempelli, A. Giacomino, S. Daniele, Modified screen printed electrode suitable for electrochemical measurements in gas phase, Anal. Chem. 92 (5) (2020) 3689–3696, https://doi.org/10.1021/acs.analchem.9b04818.
[19] N. Chantipmanee, P.C. Hauser, Determination of tobramycin in eye drops with an open-source hardware ion mobility spectrometer, Anal. Bioanal. Chem. 414 (2022) 4059–4066, https://doi.org/10.1007/s00216-022-04050-2.
[20] D.N. Barreto, G. Martins, P.C. Hauser, B. Mizaikoff, J.F. da Silveira Petruci, Reagent-less and sub-minute quantification of sulfite in food samples using substrate-integrated hollow waveguide gas sensors coupled to deep-UV LED, Anal. Chim. Acta 1236 (2022) 340596, https://doi.org/10.1016/j.aca.2022.340596.
[21] J. Roales, F.G. Moscoso, A.P. Vargas, T. Lopes-Costa, J.M. Pedrosa, Colorimetric gas detection using molecular devices and an RGB sensor, Chemosensors 11 (2023) 92, https://doi.org/10.3390/chemosensors11020092.
[22] C. Grazioli, N. Dossi, F. Cesaro, R. Svigelj, R. Toniolo, G. Bontempelli, A 3D printed Do-It-Yourself miniaturized device with a sensor responsive at six different wavelengths for reflectance measurements on paper-based supports, Microchem. J. 182 (2022) 107857, https://doi.org/10.1016/j.microc.2022.107857.
[23] K. Laganovska, A. Zolotarjovs, M. Vázquez, K. Mc Donnell, J. Liepins, H. Ben-Yoav, V. Karitans, K. Smits, Portable low-cost open-source wireless spectrophotometer for fast and reliable measurements, HardwareX 7 (2020) e00108, https://doi.org/10.1016/j.ohx.2020.e00108.
[24] O.I. Lipskikh, E.I. Korotkova, Y.P. Khristunova, J. Barek, B. Kratochvil, Sensors for voltammetric determination of food azo dyes-A critical review, Electrochim. Acta 260 (2018) 974–985, https://doi.org/10.1016/j.electacta.2017.12.027.
[25] E. Heidarizadi, R. Tabaraki, Simultaneous spectrophotometric determination of synthetic dyes in food samples after cloud point extraction using multiple response optimizations, Talanta 148 (2016) 237–246, https://doi.org/10.1016/j.talanta.2015.10.075.
[26] N. Dossi, R. Toniolo, F. Terzi, C. Grazioli, R. Svigelj, F. Gobbi, G. Bontempelli, A simple strategy for easily assembling 3D printed miniaturized cells suitable for simultaneous electrochemical and spectrophotometric analyses, Electroanalysis 32 (2020) 291–300. https://10.1002/elan.201900461.
[27] K. Ntrallou, H. Gika, E. Tsochatzis, Analytical and sample preparation techniques for the determination of food colorants in food matrices, Foods 9 (2020) 58, https://doi.org/10.3390/foods9010058.
[28] T. Salzillo, A. Marchetti, J. Vejpravova, P. Fanjul Bolado, C. Fontanesi, Molecular electrochemistry. An overview of a crossfield: electrochemistry/spectroscopic/theoretical integrated approach, Curr. Opin. Electrochem. 35 (2022) 101072, https://doi.org/10.1016/j.coelec.2022.101072.
[29] H.M. Murilo Facure, R.S. Andre, R.M. Cardoso, L.A. Mercante, D.S. Correa, Electrochemical and optical dual-mode detection of phenolic compounds using MnO2/GQD nanozyme, Electrochim. Acta 441 (2023) 141777, https://doi.org/10.1016/j.electacta.2022.141777.
[30] K. Yu, M. Li, H. Chai, Q. Liu, X. Hai, M. Tian, L. Qu, T. Xu, G. Zhang, X. Zhang, MOF-818 nanozyme-based colorimetric and electrochemical dual-mode smartphone sensing platform for in situ detection of H_2O_2 and H_2S released from living cells, Chem. Eng. J. 451 (2023) 138321, https://doi.org/10.1016/j.cej.2022.138321.
[31] J. Xu, B. Zhang, Y. Zhang, L. Mai, W. Hu, C.-J. Chen, J.-T. Liu, G. Zhu, Recent advances in disease diagnosis based on electrochemical-optical dual-mode detection method, Talanta 253 (2023) 124037, https://doi.org/10.1016/j.talanta.2022.124037.
[32] H. Eynaki, M. Ali Kiani, H. Golmohammadi, Nanopaper-based screen-printed electrodes: a hybrid sensing bioplatform for dual optoelectrochemical sensing applications, Nanoscale 12 (2020) 18409, https://doi.org/10.1039/d0nr03505j.
[33] F. Sekli Belaïdi, L. Farouil, L. Salvagn, P. Temple-Boyer, I. Séguya, J.L. Heully, F. Alary, E. Bedel-Pereira, J. Launay, Towards integrated multi-sensor platform using dual electrochemical and optical detection for on-site pollutant detection in water, Biosens. Bioelectron. 132 (2019) 90–96, https://doi.org/10.1016/j.bios.2019.01.065.
[34] J.H. Yoe, George R. Boyd, Patent blue V as a pH and redox indicator, Ind. Eng. Chem. Anal. 11 (1939) 492–493, https://doi.org/10.1021/ac50137a008.
[35] A.N. Chebotaver, K.V. Bevzink, D.V. Snigur, Y.R. Bazel, The brilliant blue FCF ion-molecular forms in solutions according to the spectrophotometriy data, Russ. J. Phys. Chem. A 91 (2017) 1907–1912, https://doi.org/10.1134/S0036024417100089.
[36] P. Ngamukot, T. Charoenraks, O. Chailapakul, S. Motomizu, S. Chuanuwatanakul, Cost-effective flow cell for the determination of malachite green and leucomalachite green at a boron-doped diamond thin-film electrode, Anal. Sci. 22 (2006) 111–116.
[37] N.S. Kobotaeva, E.E. Ssirotkina, E.V. Mikubaeva, Electrochemical oxidation of tritane dyes, Russ. J. Electrochem. 42 (2006) 268–271, https://doi.org/10.1134/S1023193506030104.
[38] A. Sacide, S. Toptan, Simultaneous determination of Indigotin and Ponceau-4R in food samples by using Vierordt's method, ratio spectra first order derivative and derivative UV spectrophotometry, J. Food Compos. Anal. 16 (2003) 517–530, https://doi.org/10.1016/S0889-1575(03)00022-X.
[39] V. Cerdà, P. Phansi, S. Ferreira, From mono- to multicomponent methods in UV-VIS spectrophotometric and fluorimetric quantitative analysis – a review, TrAC, Trends Anal. Chem. 157 (2022) 116772, https://doi.org/10.1016/j.trac.2022.116772.